



Advanced Qualification of Additive Manufacturing Materials Workshop

Temperature Simulations and Measurements for Process Qualification in Powder-Bed Electron Beam Additive Manufacturing

Kevin Chou

Professor

Mechanical Engineering Department
The University of Alabama

Assistant Director for Technology
Advanced Manufacturing National Program Office
U.S. Department of Commerce

July 20, 2015



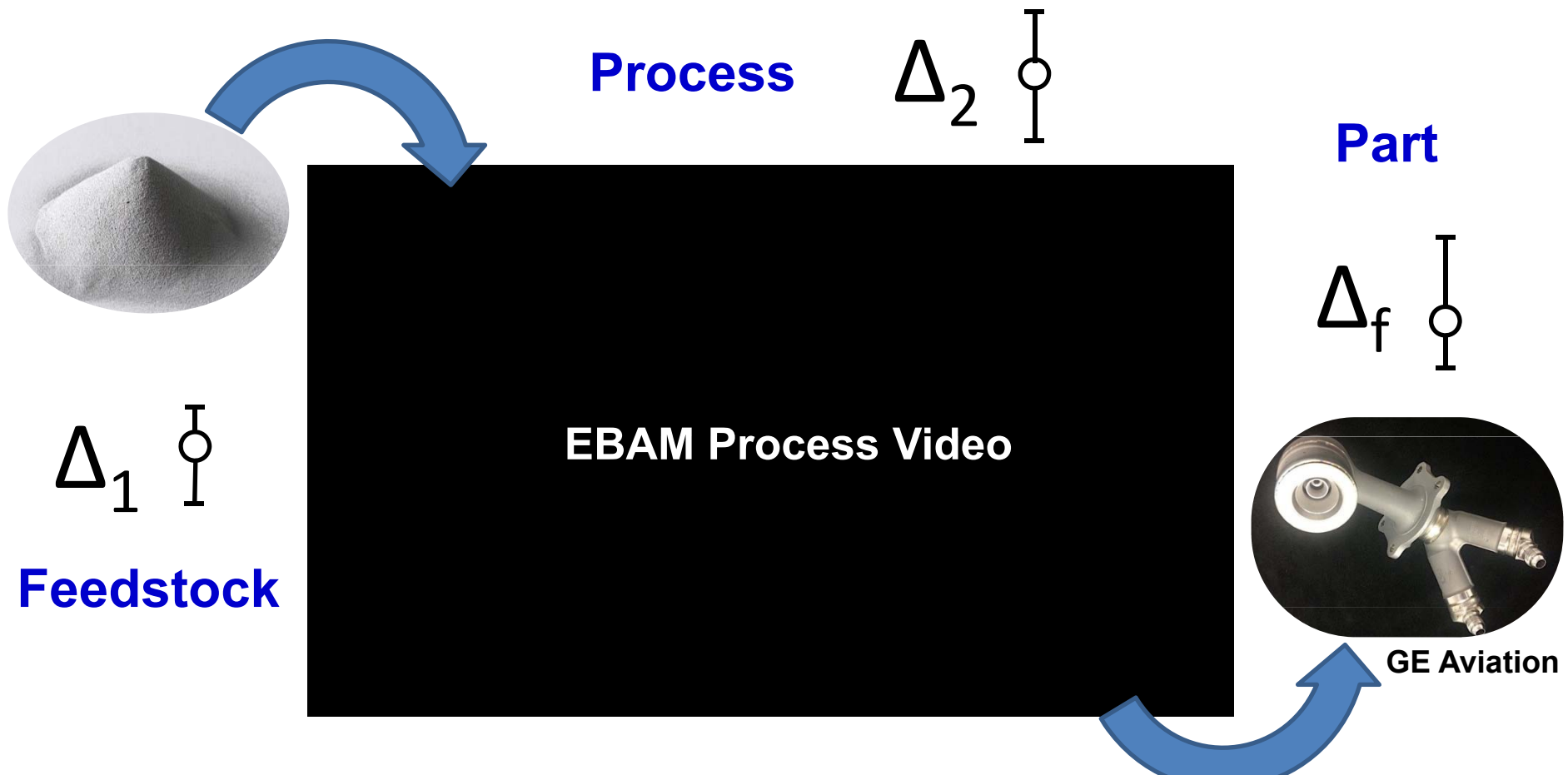
Disclaimer and Note

- The materials presented and opinions expressed in this seminar were solely from the presenter himself. They do not represent the viewpoints of The University of Alabama, nor the Advanced Manufacturing National Program Office.
- The materials presented in this seminar are mainly from the following articles.
 - Cheng, B., S. Price, J. Lydon, K. Cooper and K. Chou, "On Process Temperature in Powder-Bed Electron Beam Additive Manufacturing: Model Development and Experimental Validation," *Journal of Manufacturing Science and Engineering*, Vol. 136, No. 6, pp. 061018 (1-12), 2014.
 - Price, S., B. Cheng, J. Lydon, K. Cooper and K. Chou, "On Process Temperature in Powder-Bed Electron Beam Additive Manufacturing: Process Parameter Effects," *Journal of Manufacturing Science and Engineering*, Vol. 136, No. 6, pp. 061019 (1-10), 2014.
 - Gong, X., J. Lydon, K. Cooper, and K. Chou, "Beam Speed Effects on Ti-6Al-4V Microstructures in Electron Beam Additive Manufacturing," *Journal of Materials Research*, Vol. 29, No. 17, pp. 1951-1959, 2014.
 - Gong, X., J. Lydon, K. Cooper, and K. Chou, "Characterization of Ti-6Al-4V Powder in Electron-Beam-Melting Additive Manufacturing," *International Journal of Powder Metallurgy*, Vol. 51, No. 1, pp. 1-10, 2015.

Contact information:

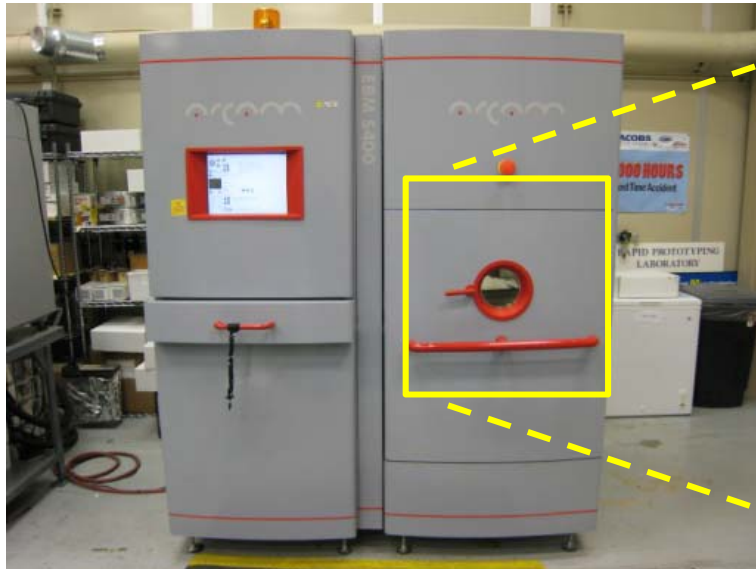
Kevin Chou, kchou@eng.ua.edu, 205-348-0044

Quality Control in AM Material and Process



EBAM System Characteristics

EBAM machine
(example, old model)



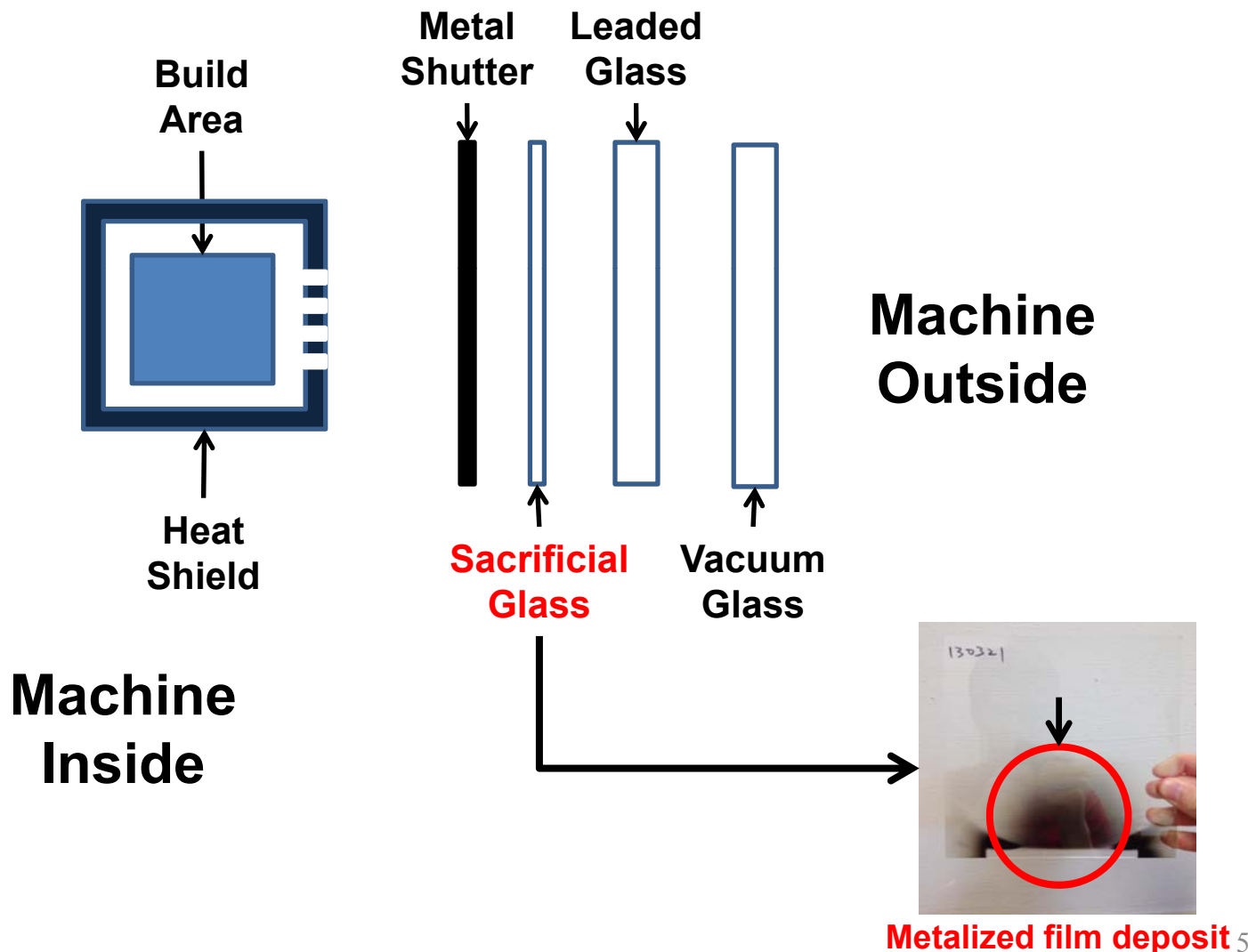
Build chamber



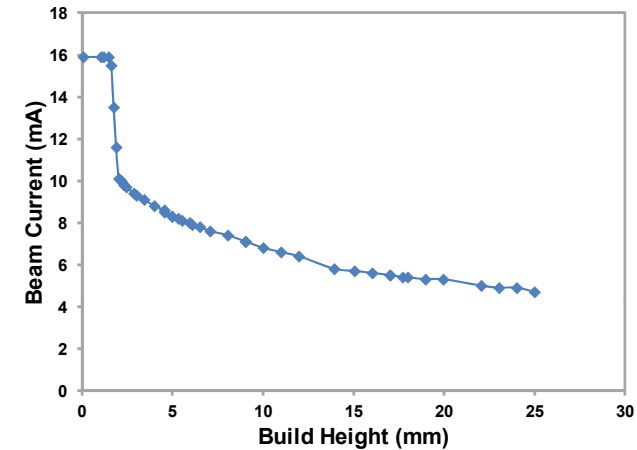
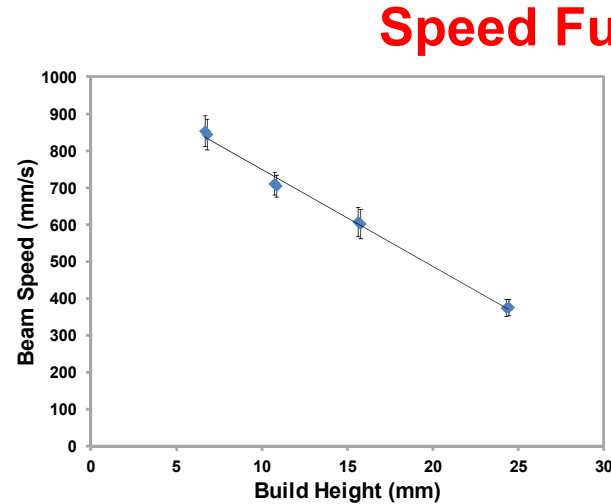
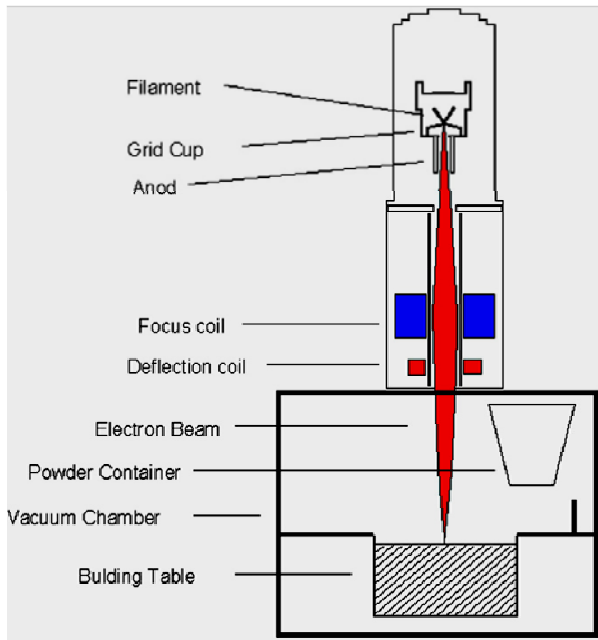
High power
60 keV electron gun
No moving part

Leaded glass
High strength glass
Heat shield
Sensor access limitation

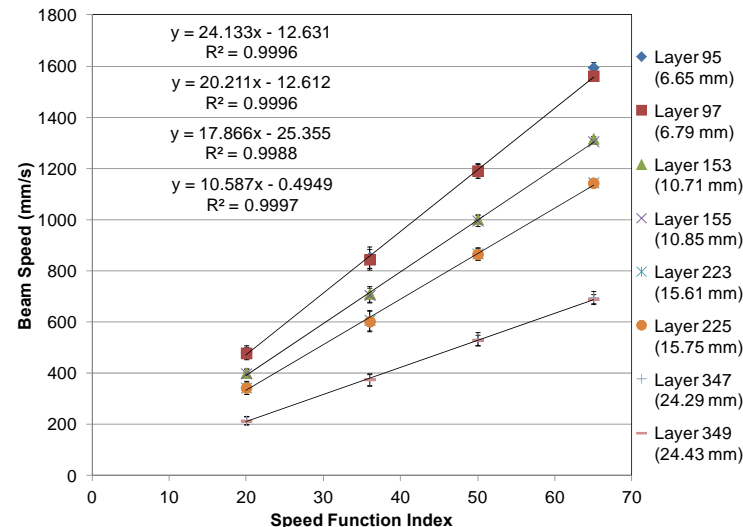
EBAM Viewport Window



EBAM Process Characteristics

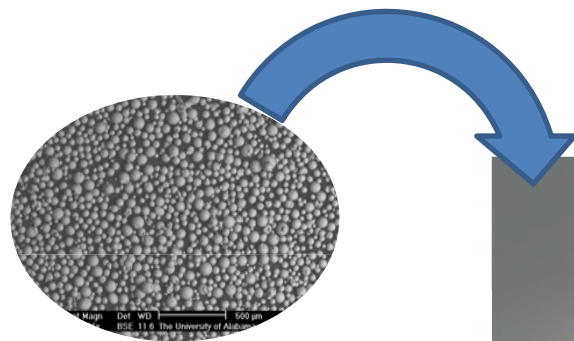


Beam Speed = function (SF, height)



Vacuum (little He)
Pre-heating, sintering
Warm process ($> \sim 650^\circ\text{C}$)
High scanning speed
Process parameters change through the build
Metalizing film
Slow post-process cooling

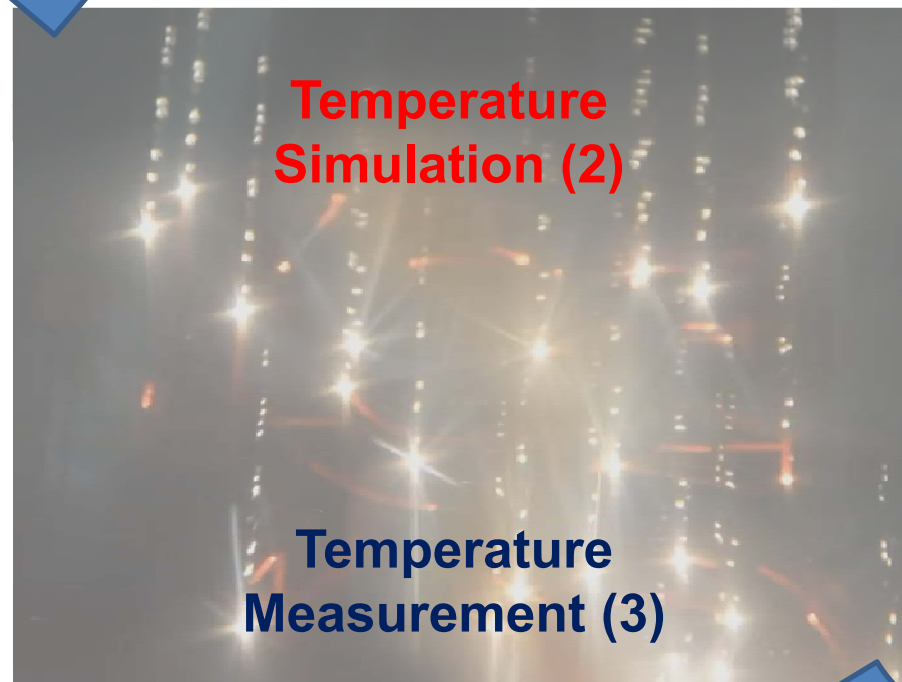
EBAM Process/Material Studies



Powder-Bed (1)

Ti-6Al-4V

Process Physics



AM Part (4)



(1) Feedstock Characterization



Powder-Bed Particles, Porosity

- Metallography, Micro-CT

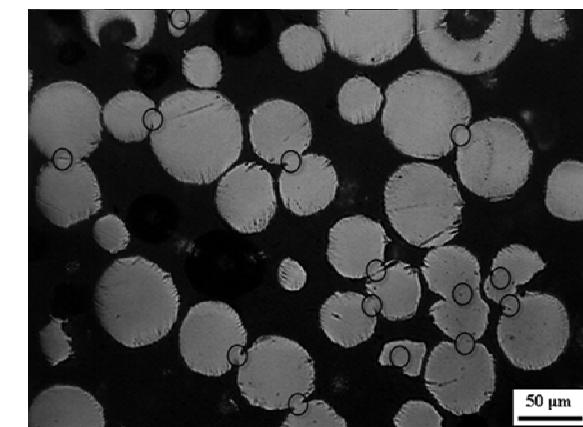
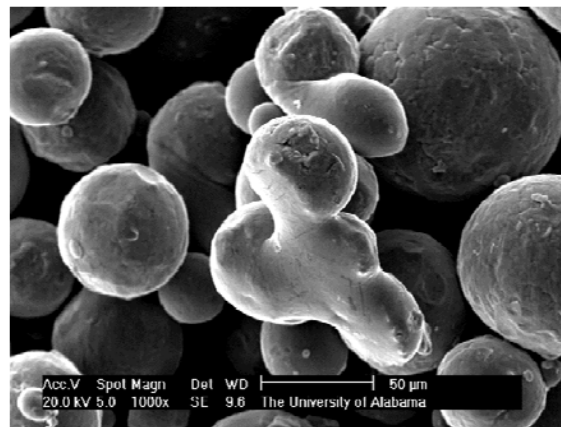
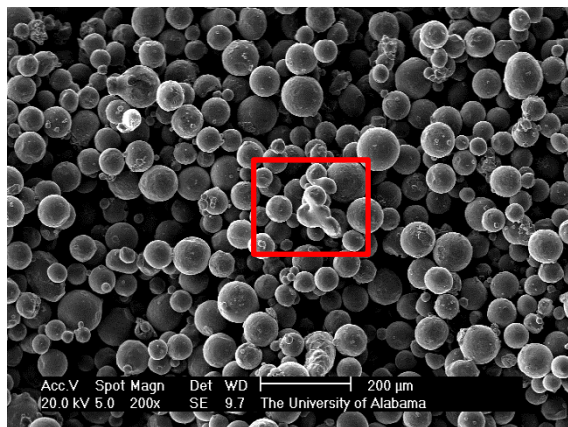
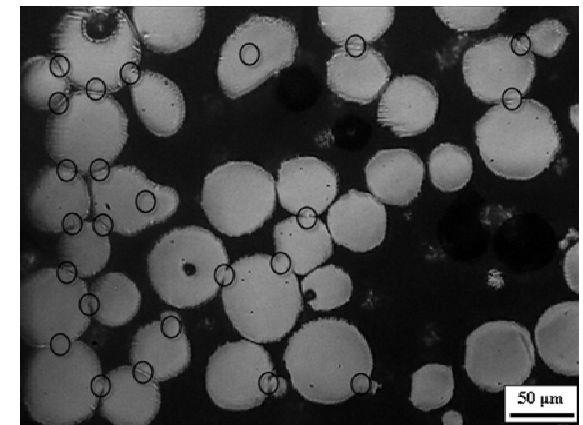
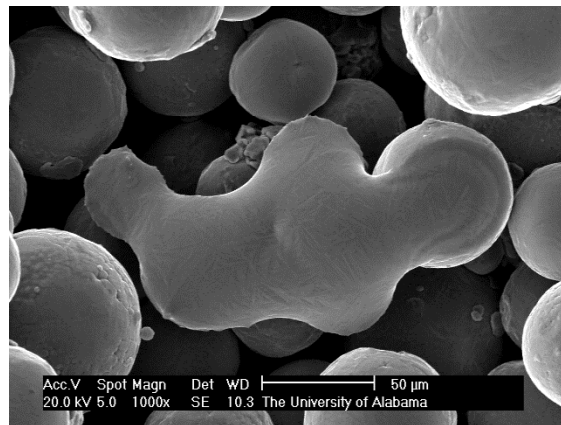
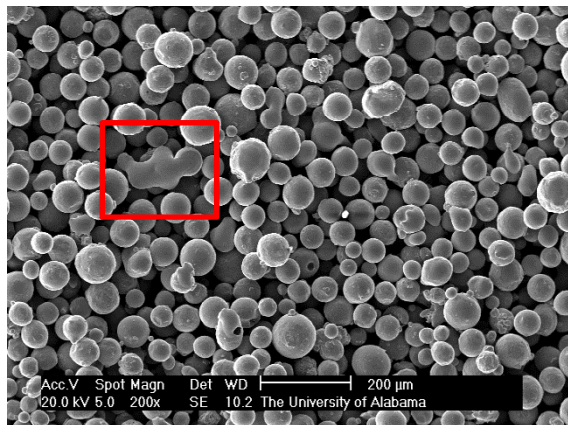


Thermal Conductivity

- Hot-Disk Thermal Analyzer

Preheated Powder

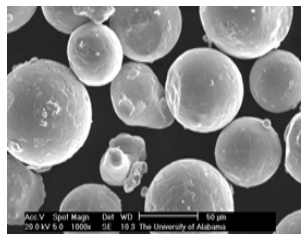
Z-plane



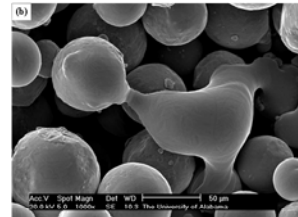
X-plane

Porosity Study - Micro-CT

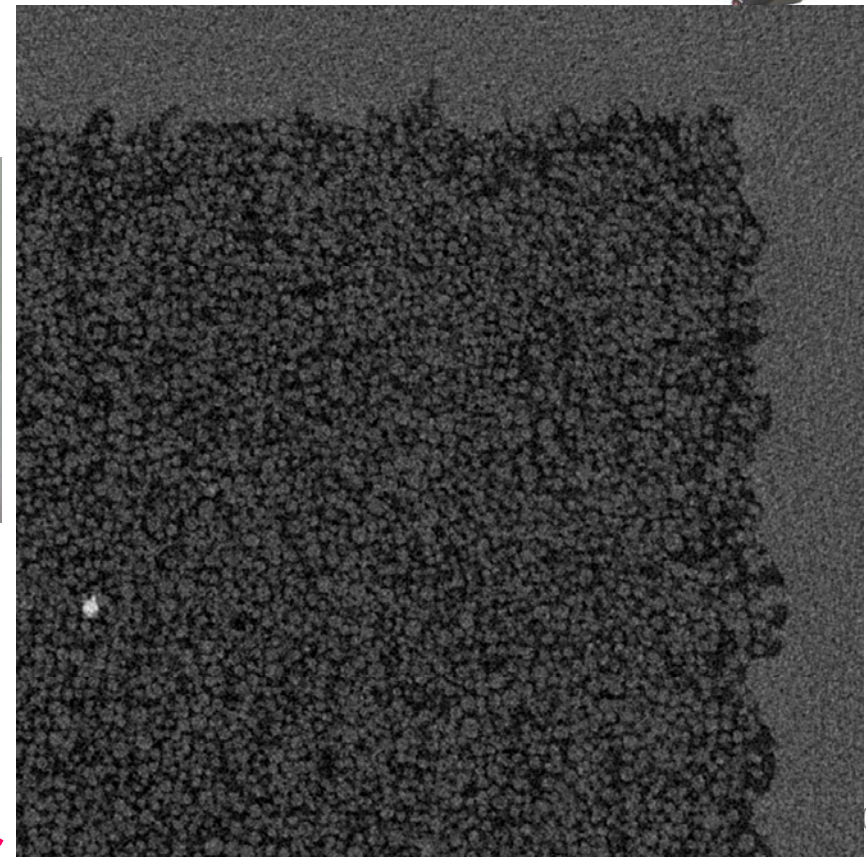
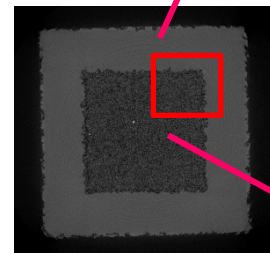
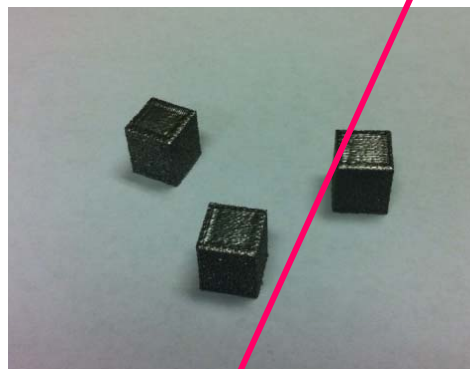
- 10 mm Ti-6Al-4V Cube (hollow)
- Skyscan 1172 Micro-CT
- Size/Porosity Distribution
 - ~ 2 μm resolution



Loose
powders

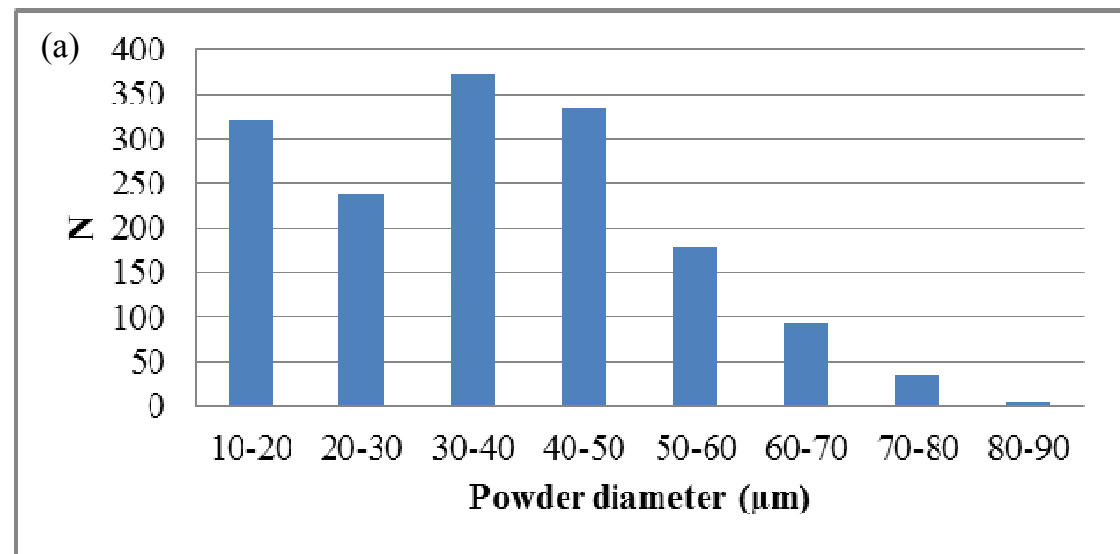
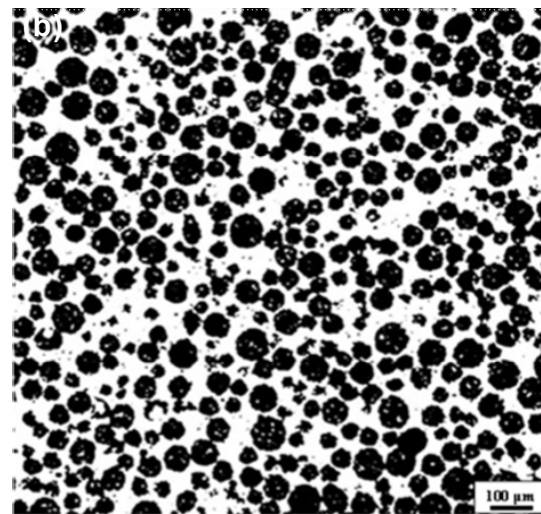


Sintered
powders



Porosity and Powder Size

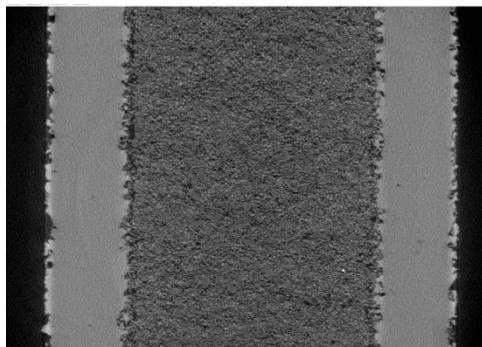
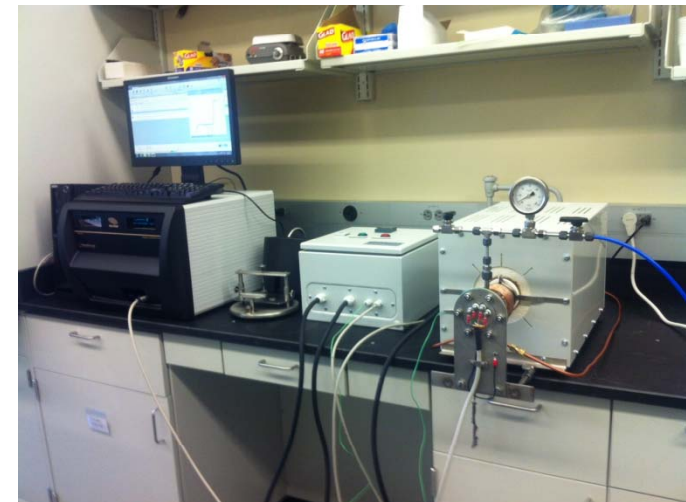
- Powder-Bed Porosity, ~ 50%
- Particle Size Distribution
Major: ~ 30 to 50 μm



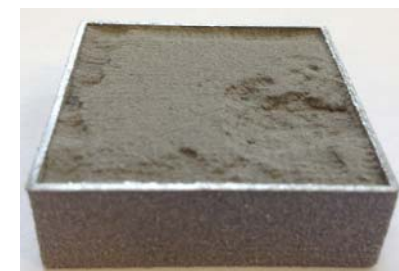
Powder Thermal Conductivity

- TPS2500 S Thermal Analyzer (Hot Disk)
 - Solid and Hollow samples

$$\frac{t_{total}}{k_{eff}} = 2 \left(\frac{t_s}{k_s} \right) + \left(\frac{t_p}{k_p} \right) \rightarrow k_p = t_p \left[\frac{t_{total}}{k_{eff}} - 2 \left(\frac{t_s}{k_s} \right) \right]^{-1}$$



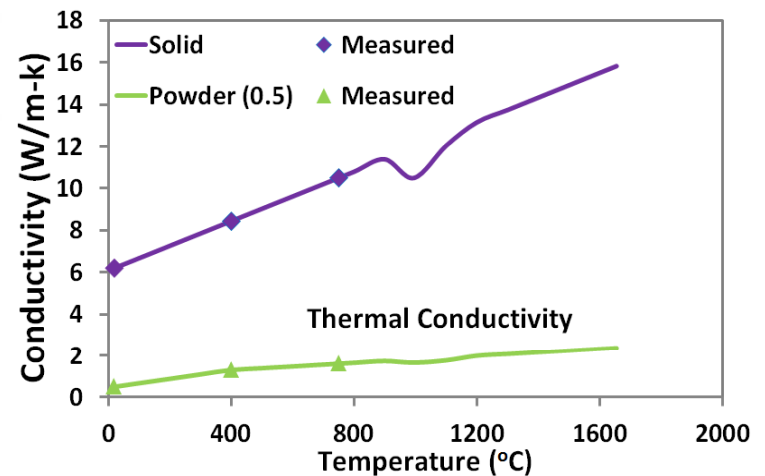
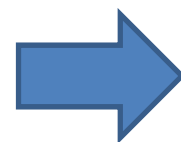
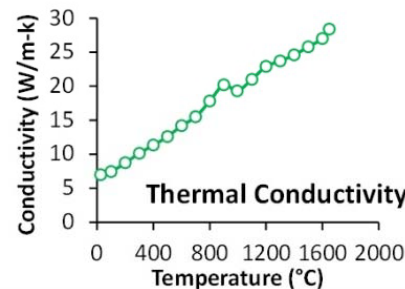
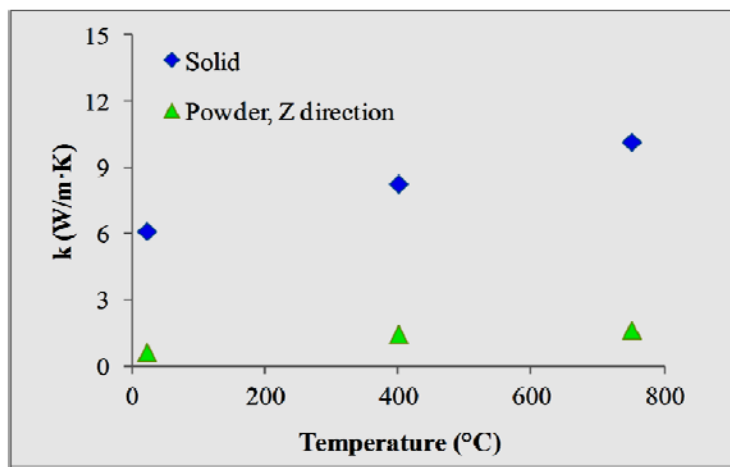
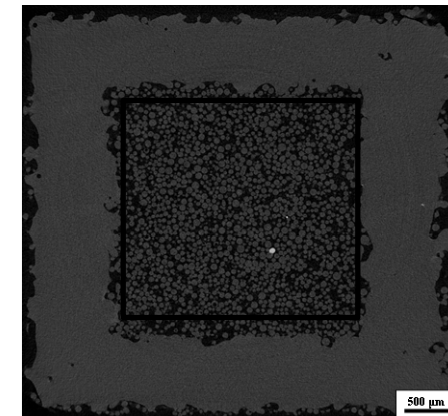
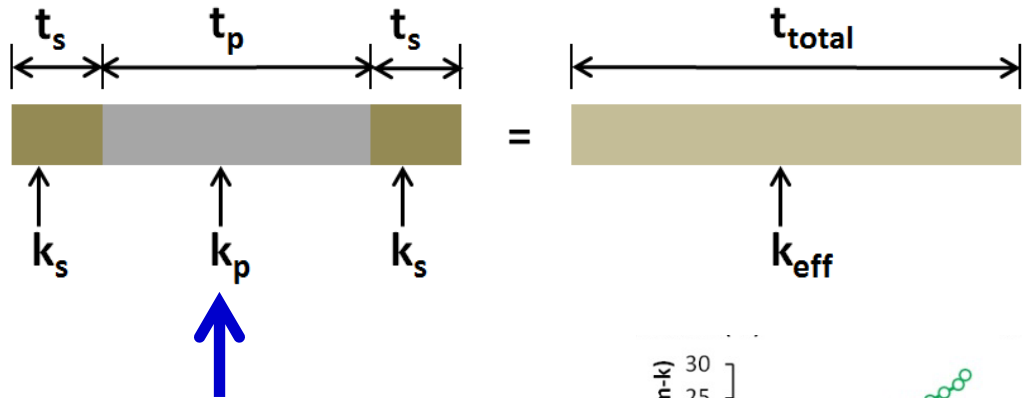
Solid vs. Hollow



Hollow sample with shell removed (1 side)

Powder Thermal Conductivity

- Sintered Powder Specimens



(2) Temperature Simulation

- Finite Element Modeling

- Heat Transfer
- Heat Source
- Material/Powder Properties
- Latent Heat of Fusion

Governing Equations

Heat Transfer

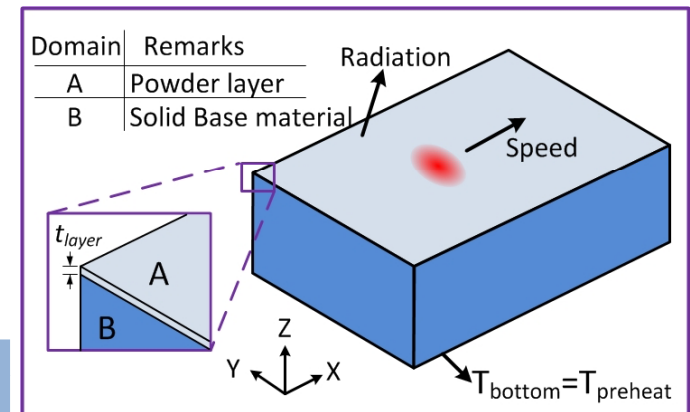
$$\nabla(k\nabla T) + \dot{Q} = \frac{\partial(\rho c_p \cdot T)}{\partial t} + v_s \frac{\partial(\rho c_p \cdot T)}{\partial x}$$

- T - Temperature
- $\dot{Q}_{(x,y,z)}$ - Absorbed heat flux
- c - Specific heat capacity
- ρ - Density
- λ - Thermal conductivity
- v_s - Constant speed of the moving heat source



Assumptions:

- Heat Conduction
- Negligible molten flow within molten pool
- Radiation considered as boundary condition
- Uniform temperature as the part initial temperature



Latent Heat of Fusion

$$\Delta H(T) = \int cdT + L_f f$$

$$f = \begin{cases} 0 & T < T_s, \\ \frac{T - T_s}{T_L - T_s} & T_s \leq T \leq T_L, \\ 1 & T > T_L \end{cases}$$

- ΔH_f - latent heat of fusion
- T_l - liquidus temperature
- T_s - solidus temperature
- f_s - solid fraction

Heat Source Equations

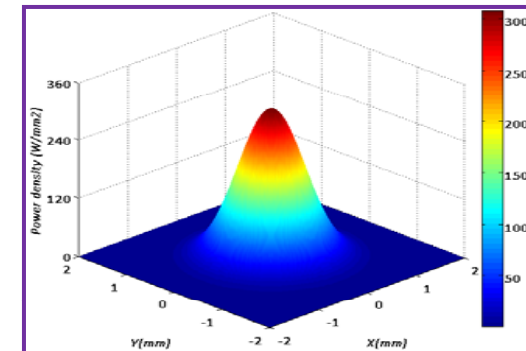
Intensity distribution: a conical source:

- Horizontal – Gaussian distribution
- Vertical – Decaying with increasing of penetration depth

$$\dot{Q}_{(x,y,z)} = \eta \times \frac{H_s \times I_z}{S}$$

$$I_z = \frac{1}{0.75} \left(-2.25 \left(\frac{z}{S} \right)^2 + 1.5 \left(\frac{z}{S} \right) + 0.75 \right)$$

$$H_s = \frac{2U I_b}{\pi \Phi_E^2} \exp \left\{ -\frac{2 \left[(x - x_s)^2 + (y - y_s)^2 \right]}{\Phi_E^2} \right\}$$



η - electron beam efficiency coefficient

U - voltage

I_b - current

S - penetration depth

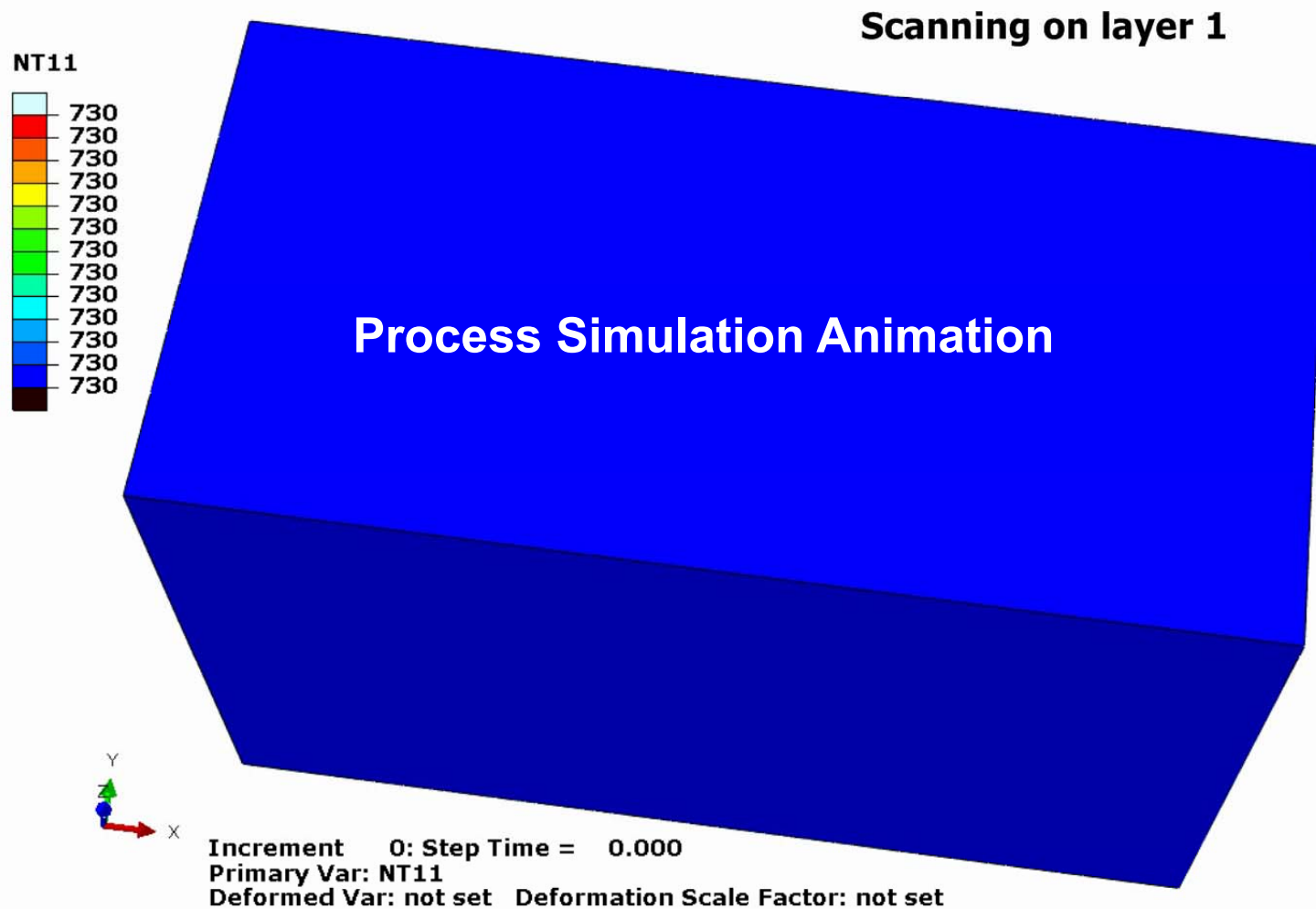
Φ_E - beam diameter

x_s, y_s - horizontal position of heat source center

H_s - Gaussian heat source, Cline and Anthony

I_z - penetration function, Zäh and Lutzmann

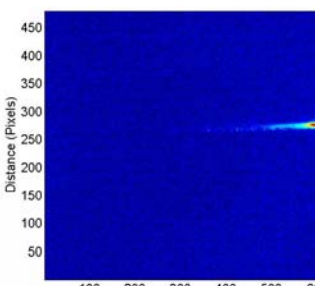
Simulation Example



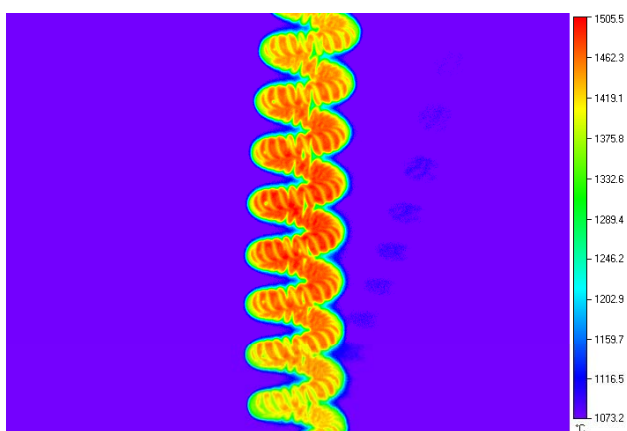
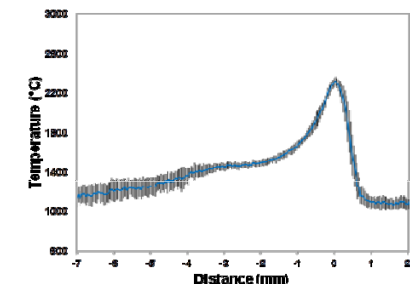
(3) Temperature Measurements

- Near IR Thermography

- Spectral Range**
- Build Area View Access**
- Resolutions (Spatial/Temporal)**
- Emissivity**
- Transmission Loss**



EBAM Temperature Measurements

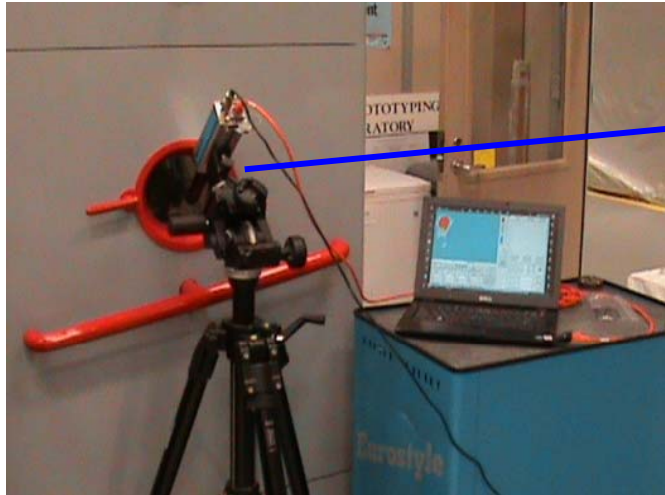


Near Infrared Thermal Imager

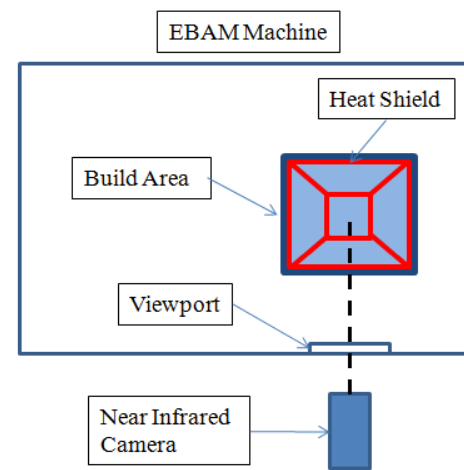
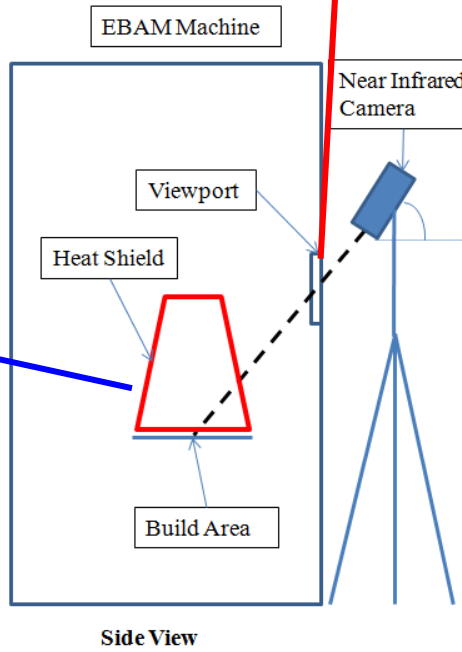
- LumaSense MCS640
- Spectral Range: 780 – 1080 nm
- 640 by 480 FPA (Amorphous Si based)
- Temperature Range: 600 to 3000 °C (3 domains)
- Frame Rate: Max. 60 Hz
- Lens: ~ 500 mm Focal Distance
- View Area: 32 mm by 24 mm
- Spatial Resolution: ~ 50 µm

Challenges:
Emissivity and Transmission

Measurement Setup

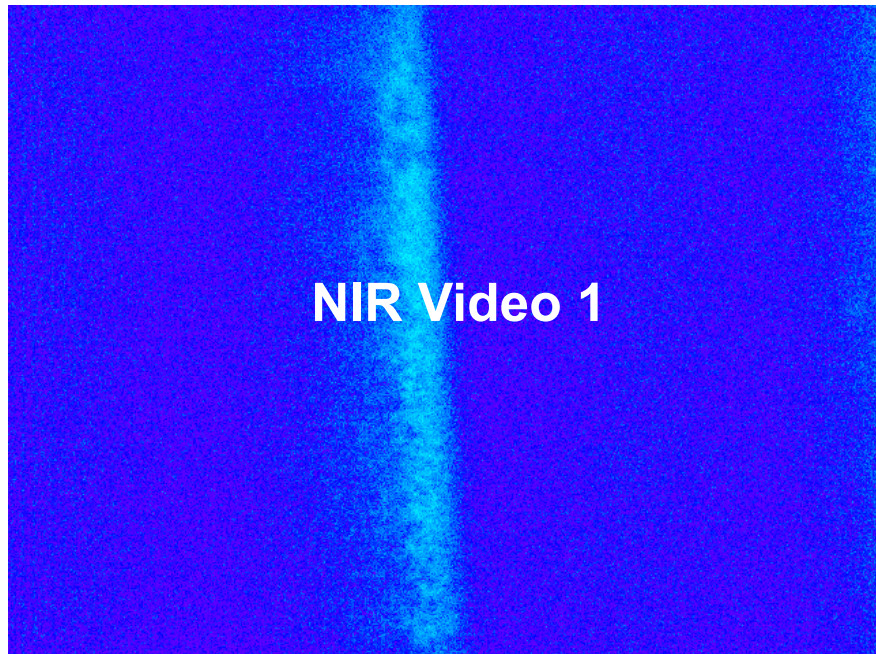


Emissivity (Single Setting, Estimated)
Transmission (Calibrated, 3 Ranges,
with Glasses)

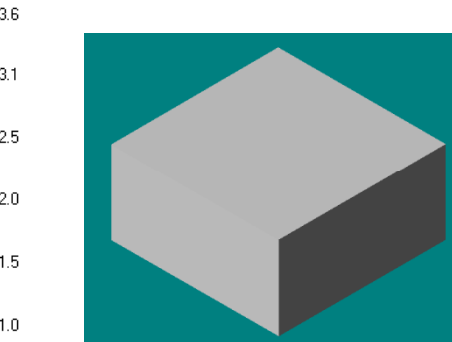


Heat shield

NIR Video Examples

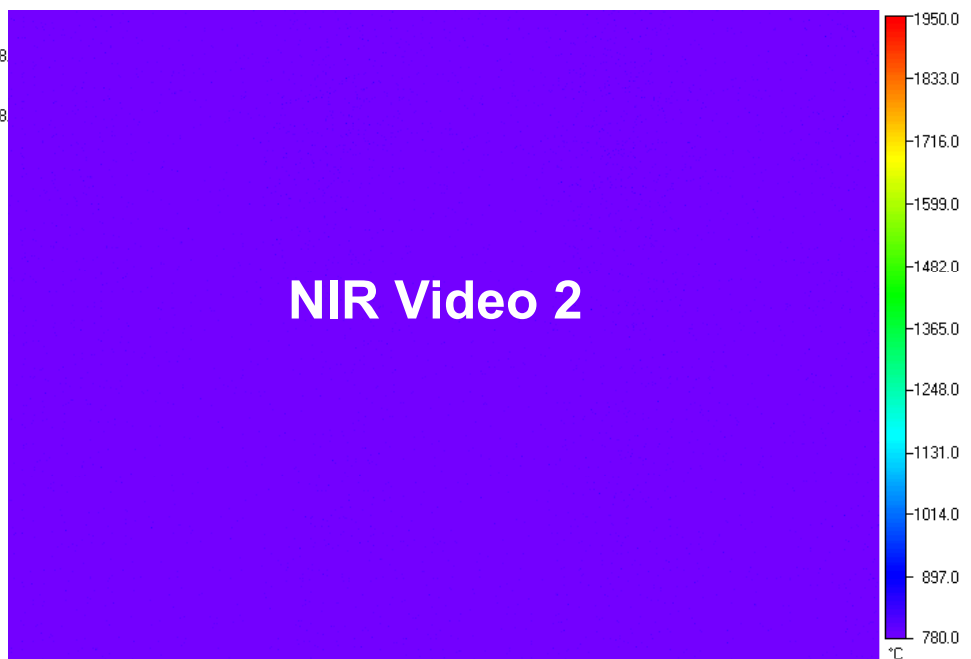


Medium Temperature Range

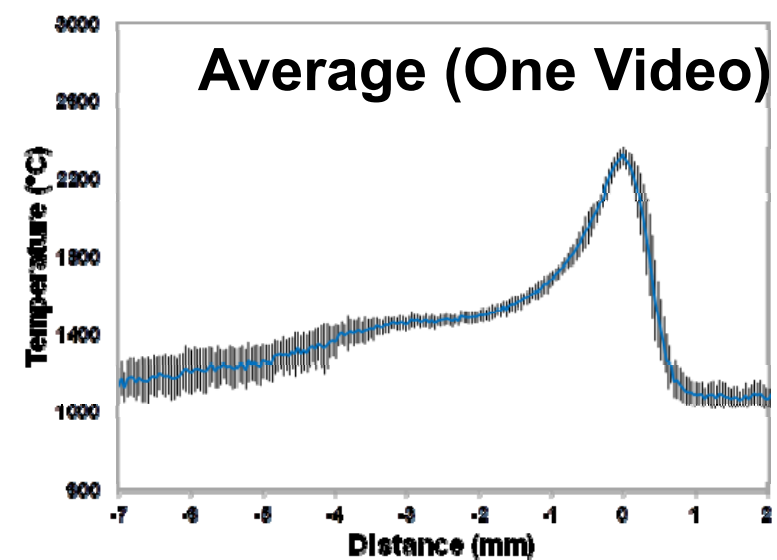
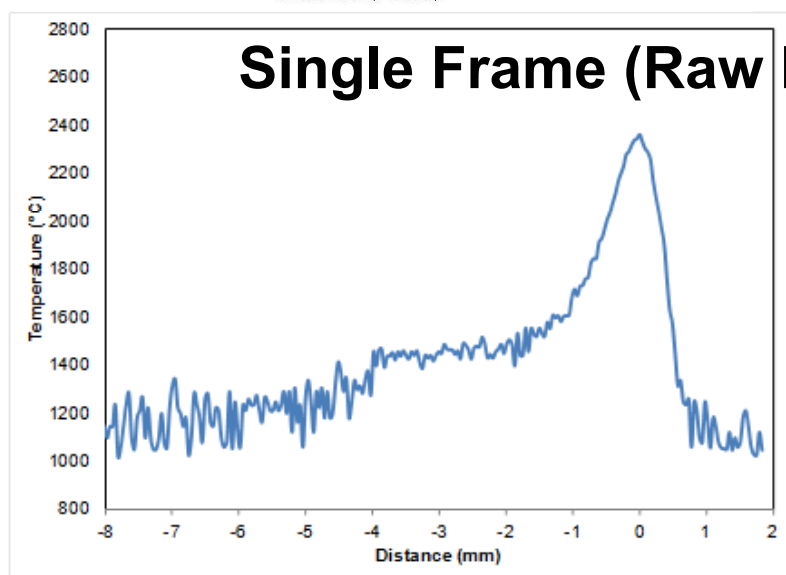
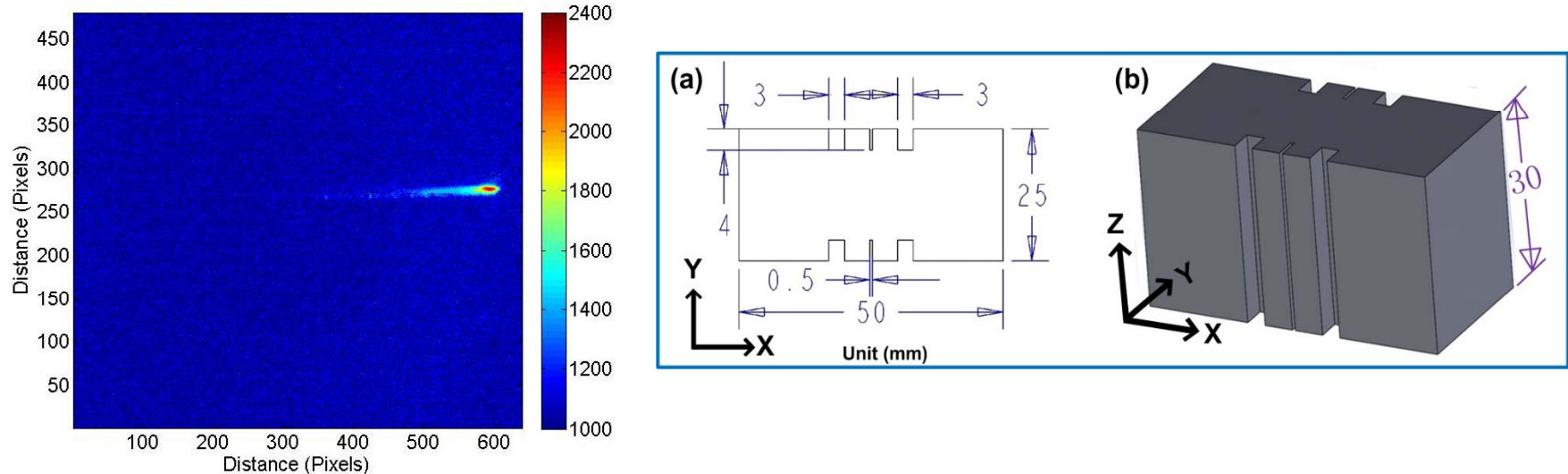


Build model:
25. 4 mm square block

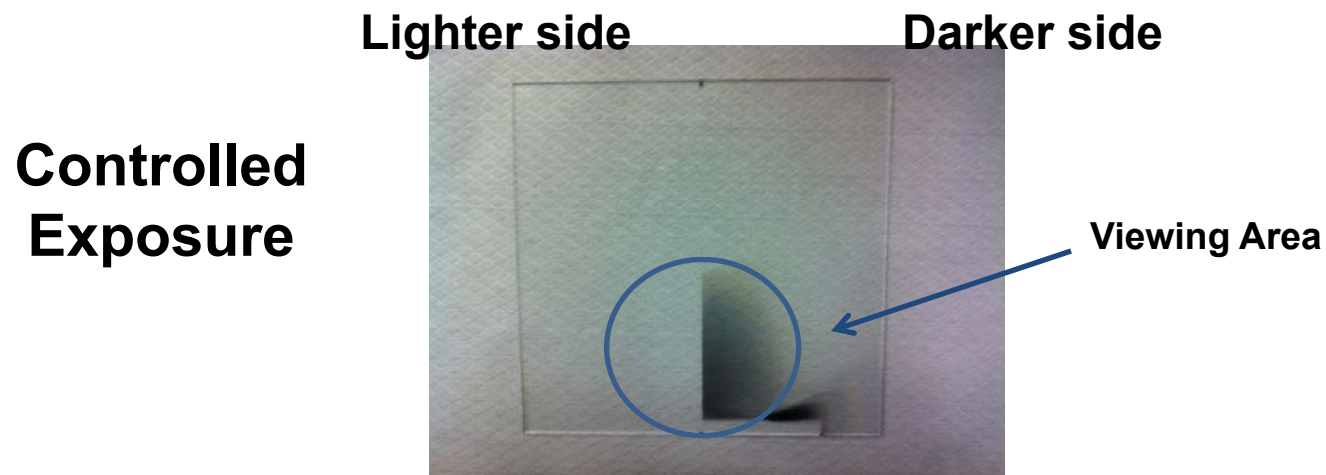
High Temperature Range



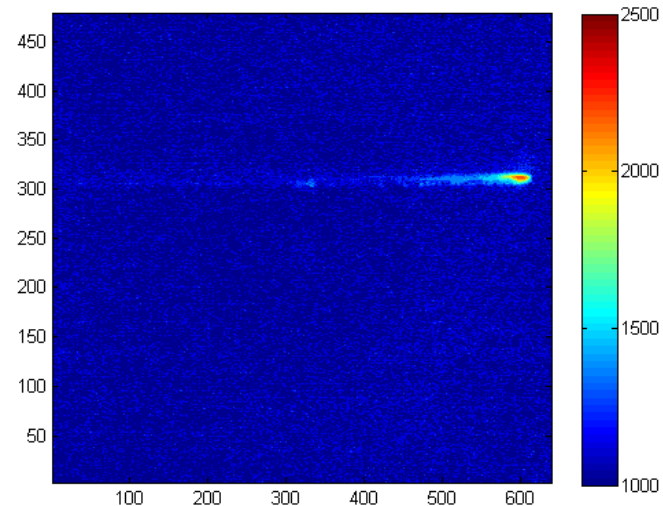
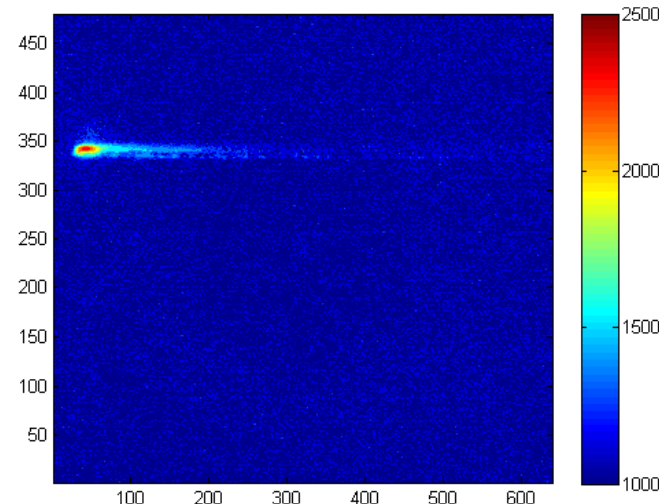
Temperature Profile Analysis (Hatch Melt)



Transmission Loss Study

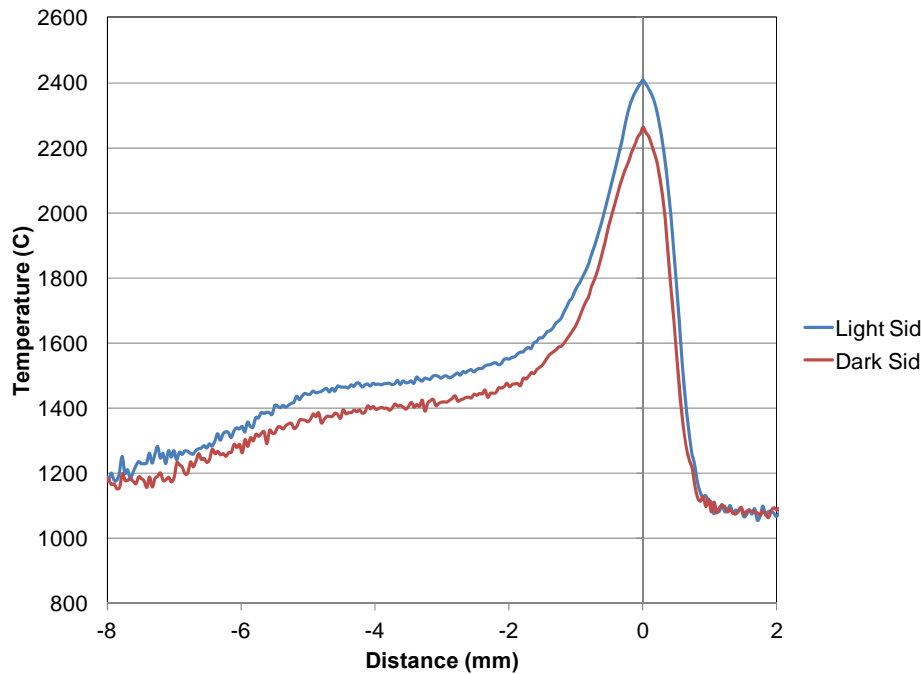


Sacrificial glass with two levels of metallization.

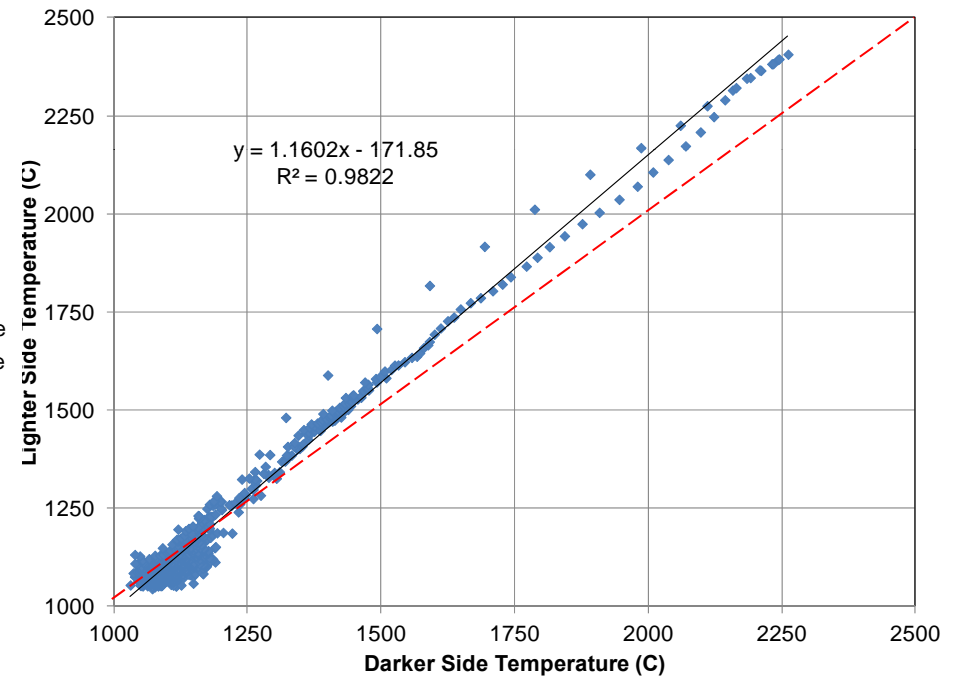


Controlled Exposure Experiment

Temperature Profiles Observed Through Different Levels of Metallization



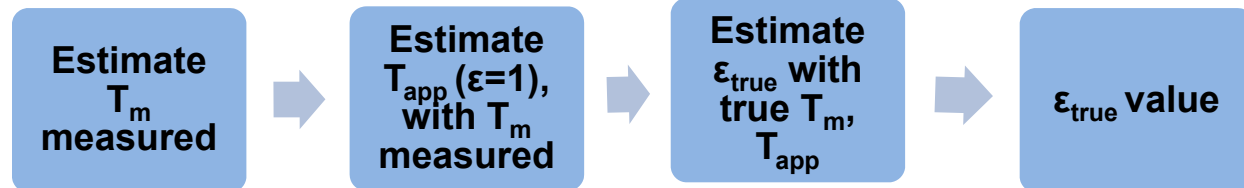
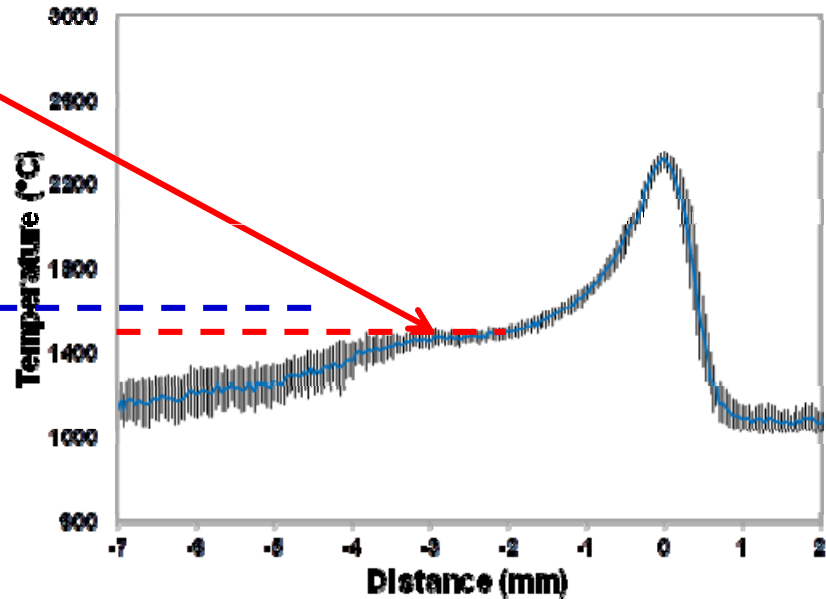
Average Temperature Profiles
(6.37 mm Build Height)



Relationship Between
Temperatures Observed Through
Different Levels of Metallization

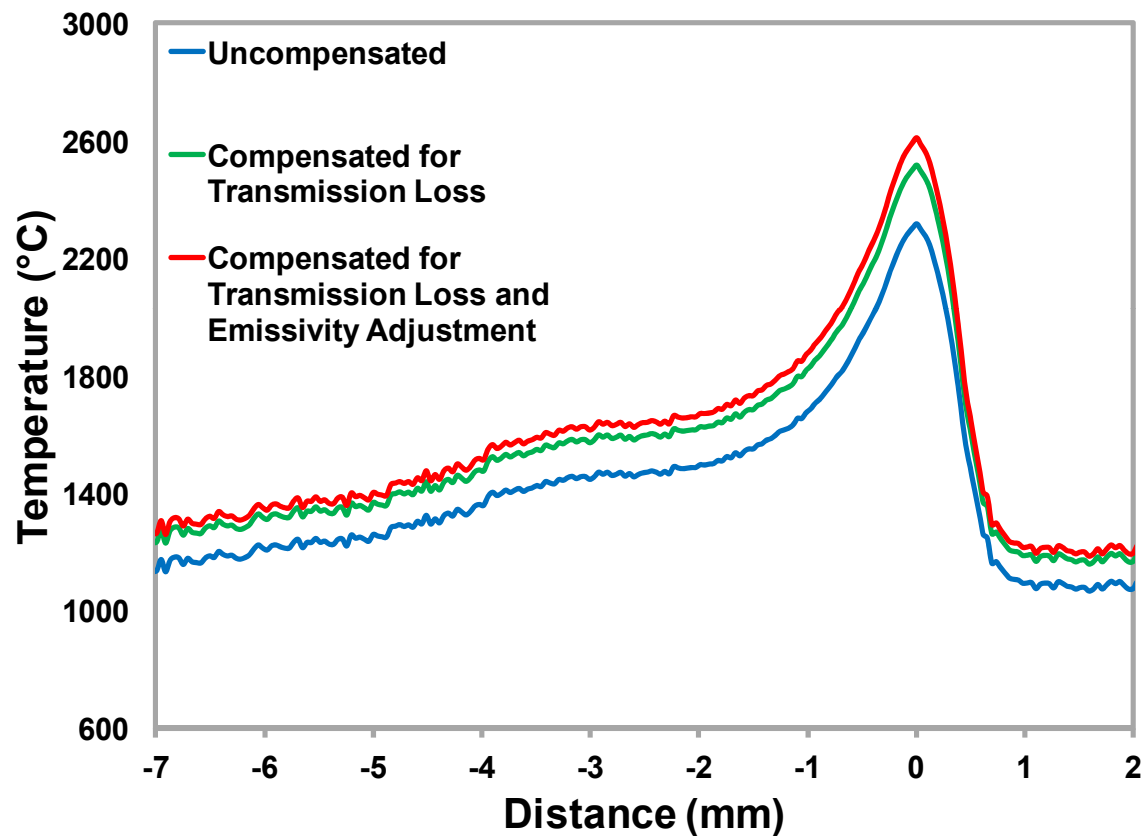
Molten State Emissivity Estimate

1. Identify **Measured Liquidus Temperature**
2. Solve for **Apparent Liquidus Temperature**, (function of measured liquidus temperature, assumed emissivity, etc.)
3. Solve for **True Emissivity**, (function of **True Liquidus Temperature**, **Apparent Liquidus Temperature**, etc.)



Estimated molten pool ϵ : ~0.28

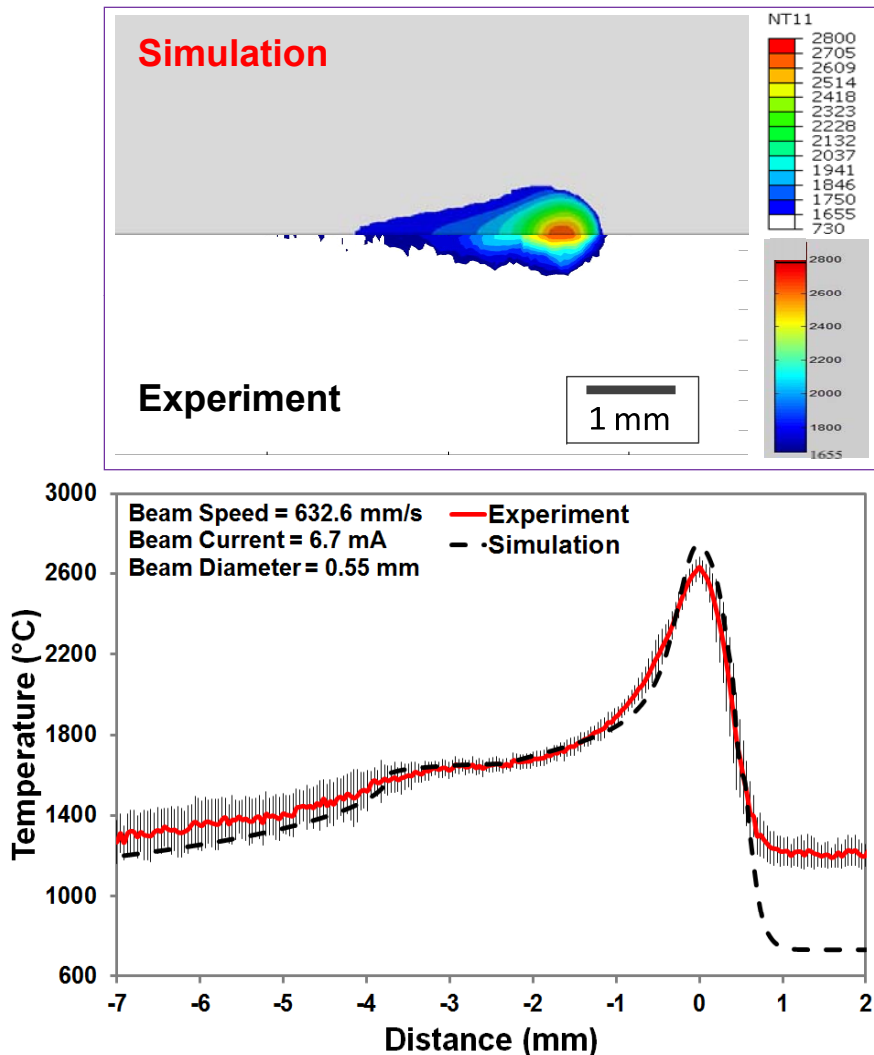
Temperature Profile Compensation



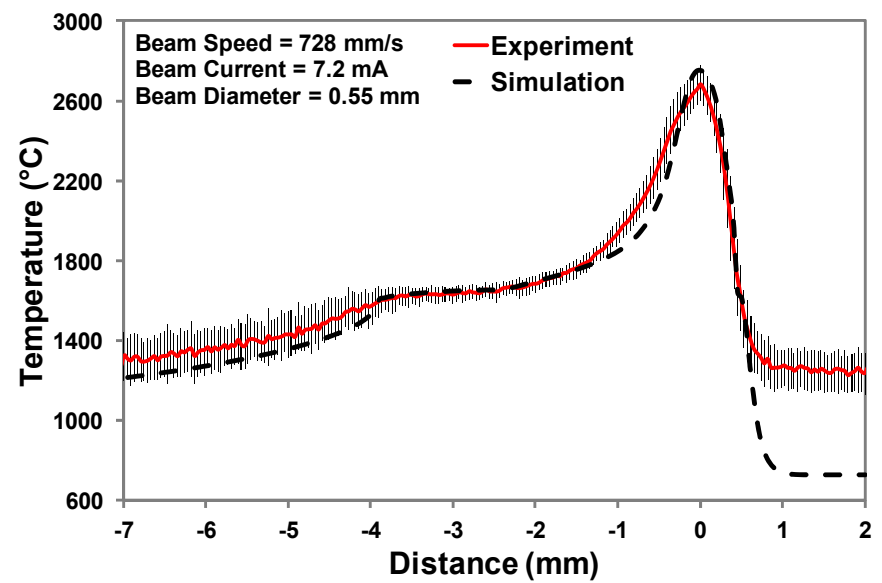
Average Temperature Profile (6.37 mm Build Height)

Simulation vs. Experiment

Set 1 Build height = 26.53 mm

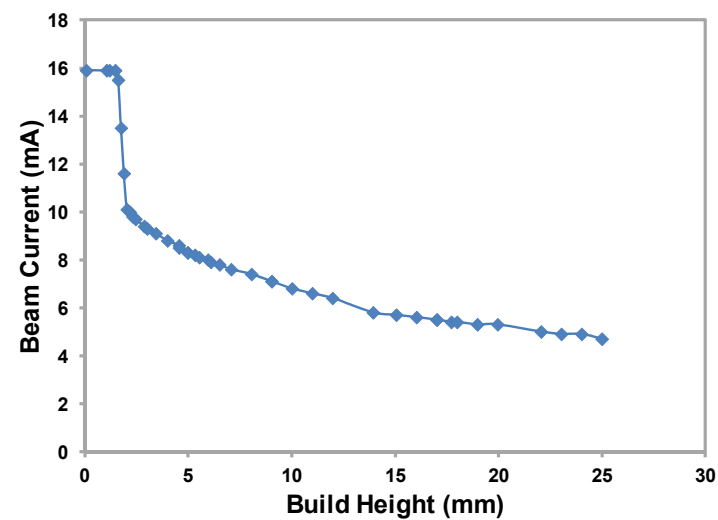
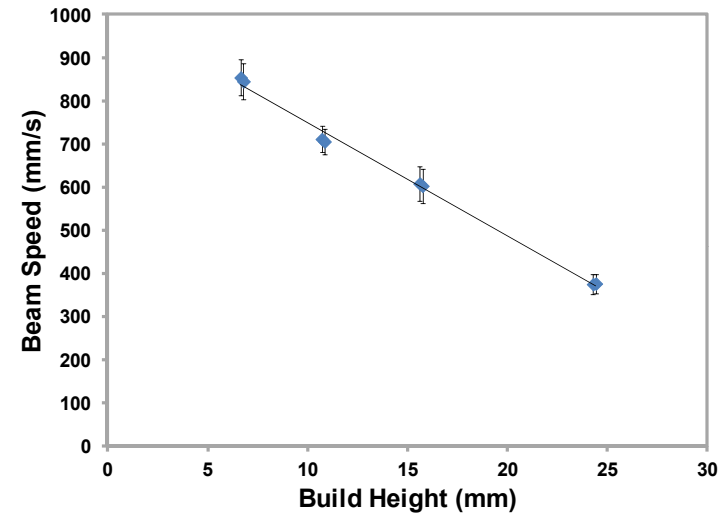
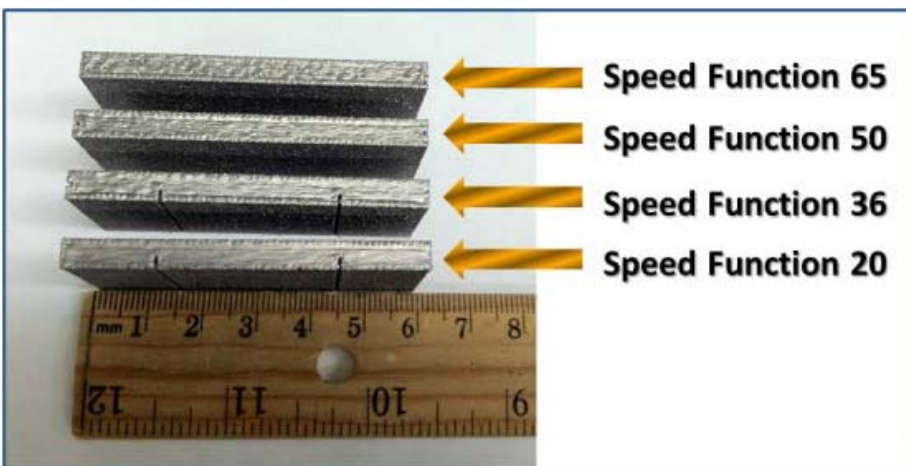


Set 2 Build height = 16.87 mm

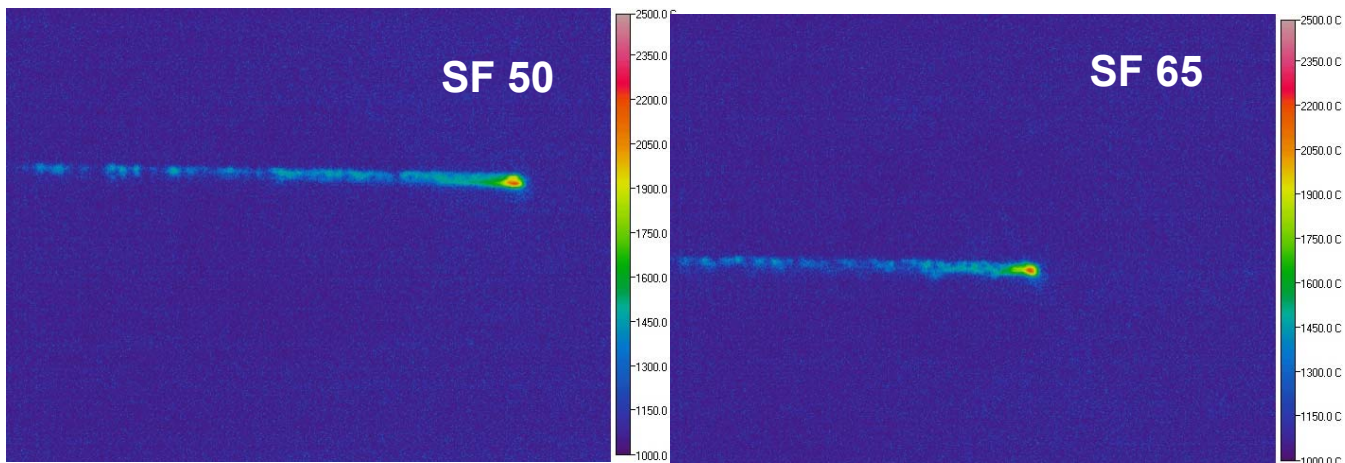
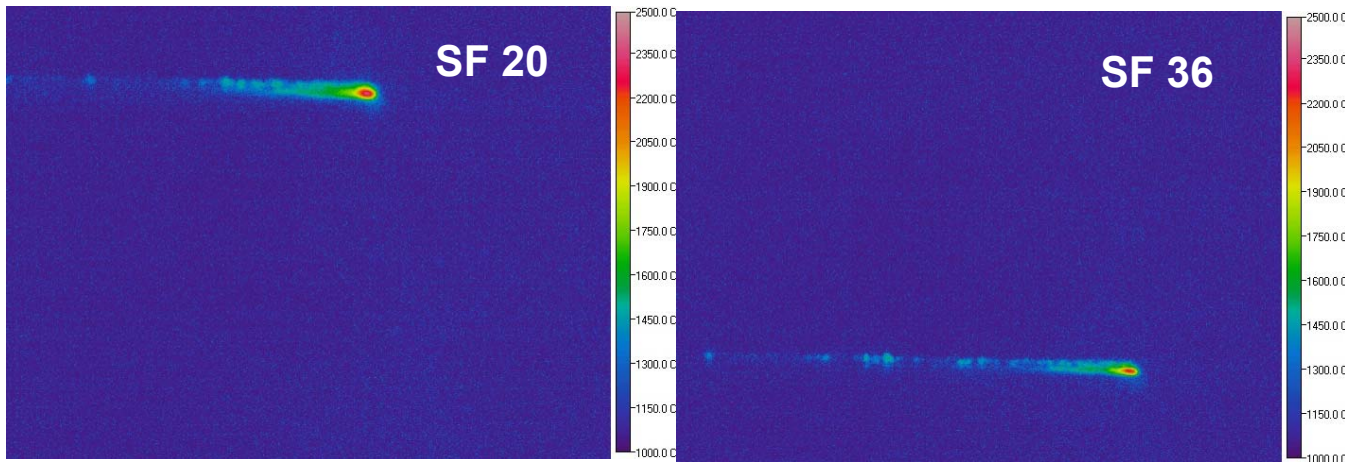


Process Parameter Effect

- Speed Function (SF) Index
 - System Setting
- Beam Speed, Current
- Tested Range
 - SF20 – SF65

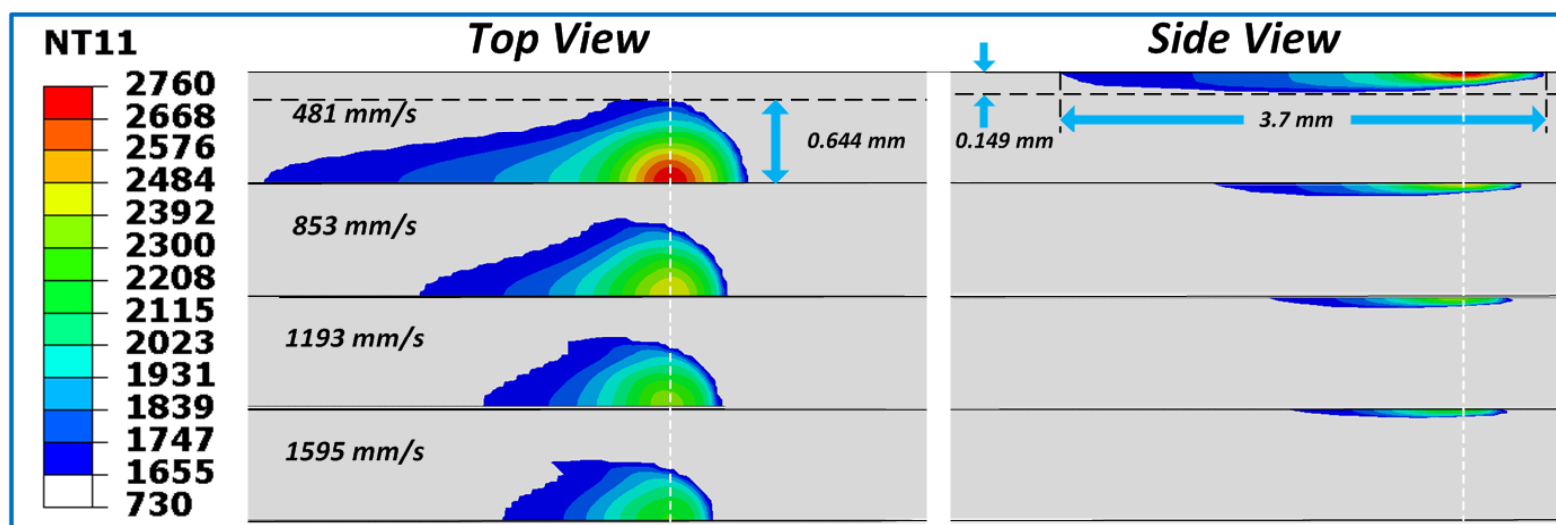
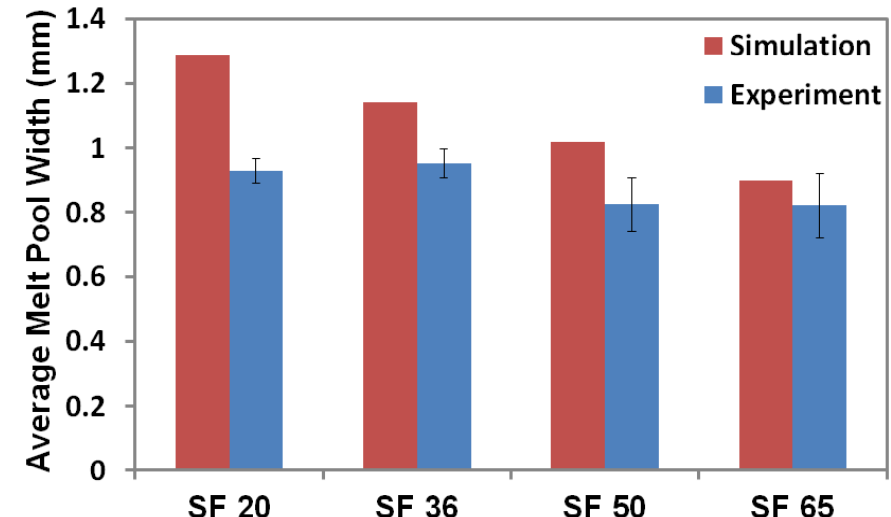
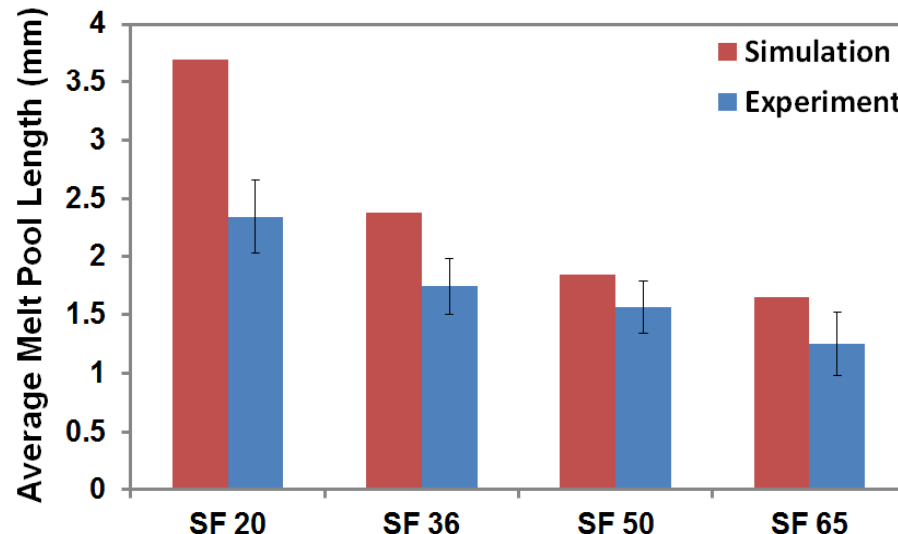


NIR Images – Different SF Indices



Melt Pool Size Comparisons

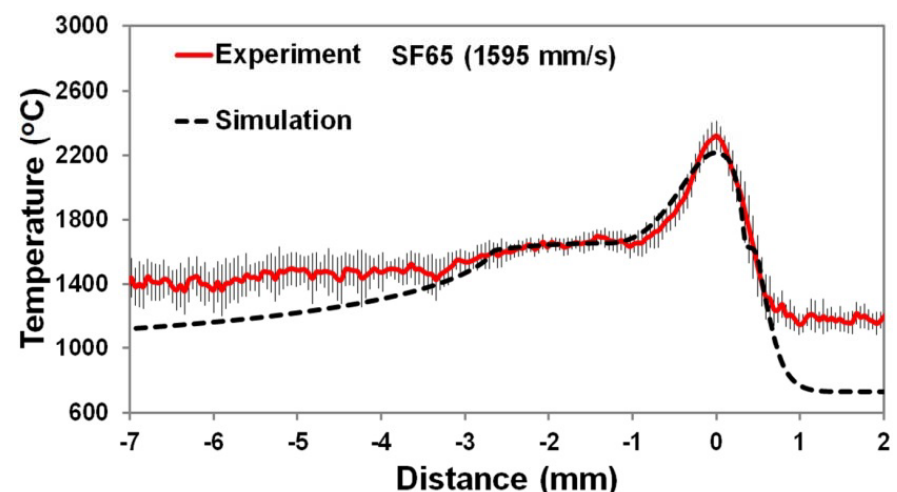
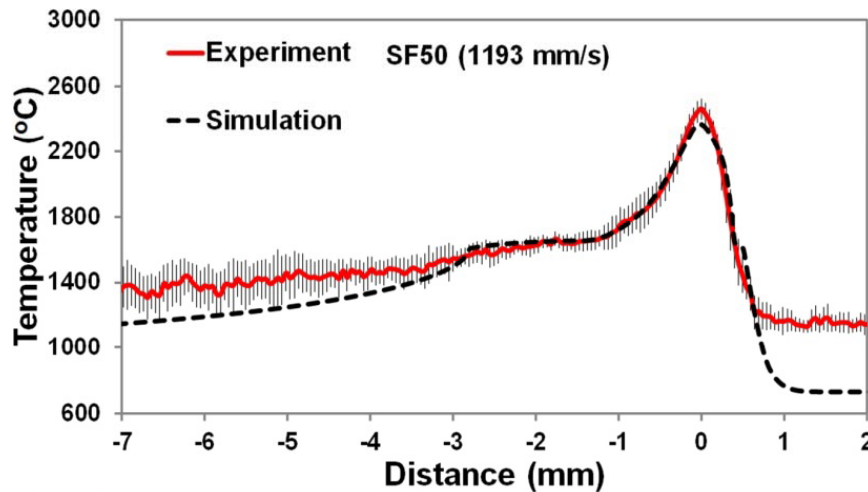
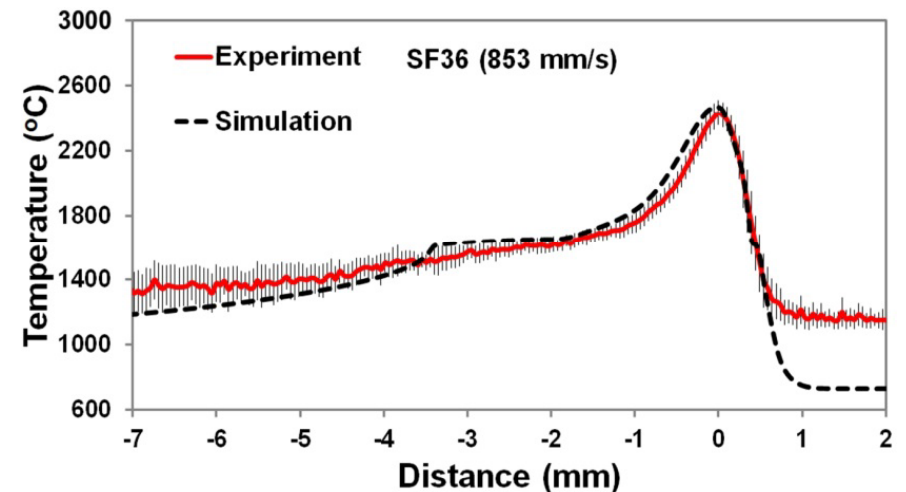
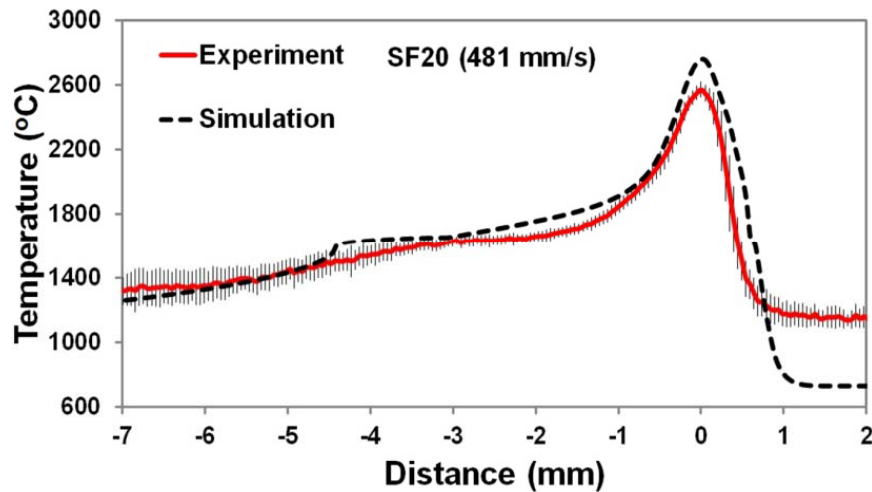
7.7 mA current, 0.65 mm diameter, 6.65 mm build height



Temperature Analysis

Beam Speed Effect

7.7 mA current, 0.65 mm diameter, 6.65 mm build height



(4) Part Characterization

-  **Microstructures (Phases, Grain Sizes)**
-  **Mechanical Properties (E, H, YS, UTS)**

EBAM Ti-6Al-4V Microstructure

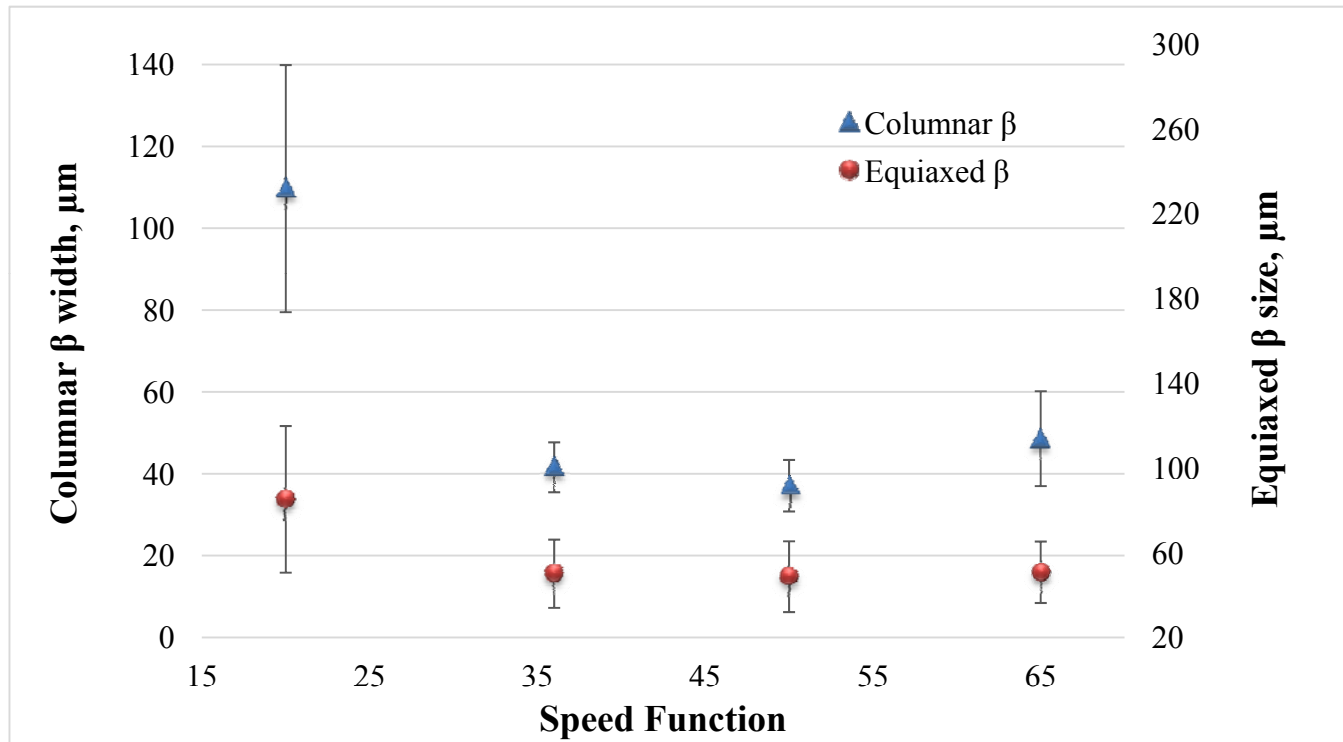


Side surface (X-plane)



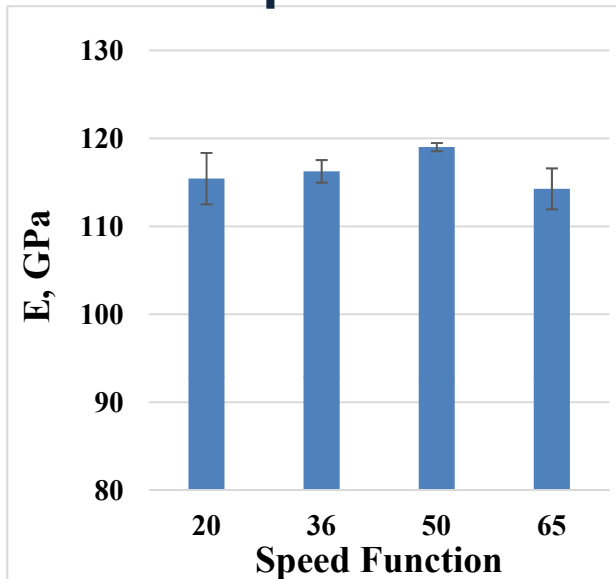
Scanning surface (Z-plane)

Process Parameter Effects

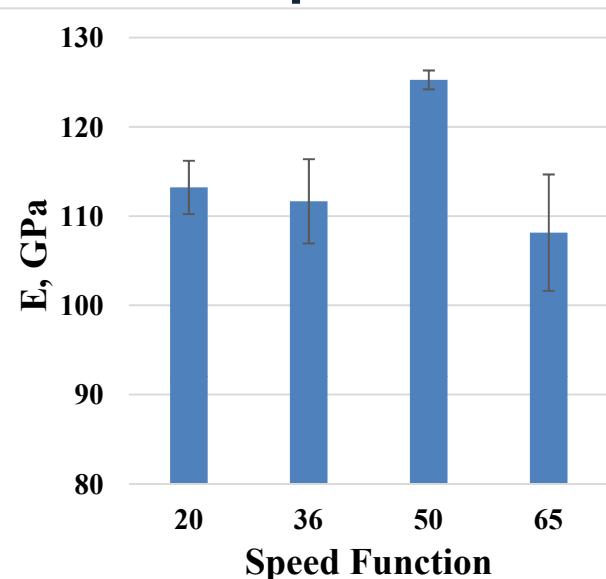


Mechanical Property (Nanoindentation)

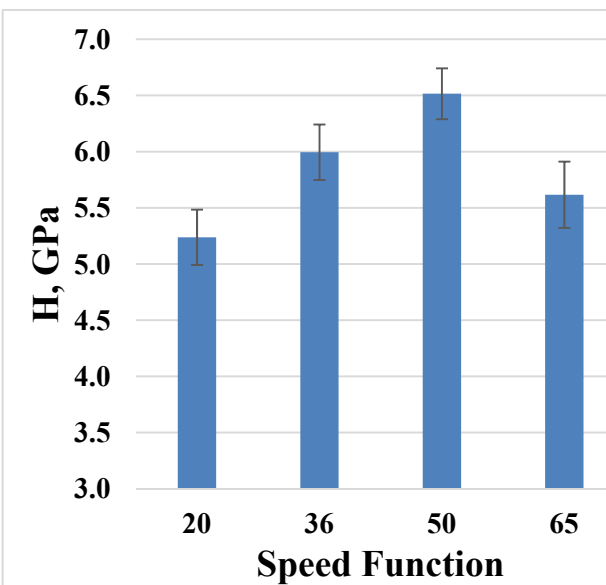
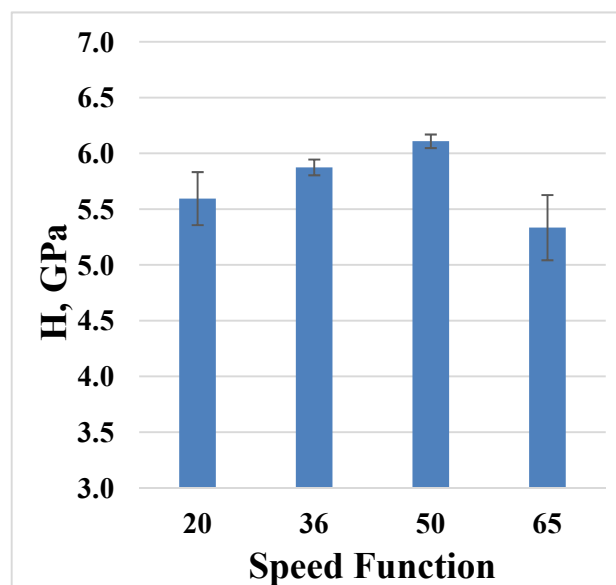
Z-plane



X-plane



Young's
modulus



Hardness

Split-Hopkinson Bar Testing

(P. Allison)

- Uniaxial Tensile, Quasi-static and Dynamic
- Mechanical Behavior

